Journal of Radiation Research, 2013, 54, i69–i76
doi: 10.1093/jrr/rrt038

Analysis of inter- and intrafraction accuracy of a commercial thermoplastic mask system used for image-guided particle radiation therapy

Dante AMELIO[1,2,*], Marcus WINTER[3], Daniel HABERMEHL[1], Oliver JÄKEL[3], Jurgen DEBUS[1] and Stephanie E. COMBS[1]

[1]Department of Radiation Oncology, University Hospital of Heidelberg, Heidelberg, Germany
[2]ATreP, Provincial Agency for Proton Therapy, Via F.lli Perini 181, 38122 Trento, Italy
[3]Department of Medical Physics, Heidelberg Ion Therapy Center (HIT), Im Neuenheimer Feld 400, 69120 Heidelberg, Germany
*Corresponding author. ATreP, Provincial Agency for Proton Therapy, Via F.lli Perini 181, 38122 Trento, Italy.
Tel: +39-461-390-409; Fax: + 39-461-397-728; Email: amelio@atrep.it

(Received 17 January 2013; revised 11 March 2013; accepted 21 March 2013)

The present paper reports and discusses the results concerning both the inter- and intrafraction accuracy achievable combining the immobilization system employed in patients with head-and-neck, brain and skull base tumors with image guidance at our particle therapy center. Moreover, we investigated the influence of intrafraction time on positioning displacements. A total of 41 patients treated between January and July 2011 represented the study population. All the patients were immobilized with a tailored commercial thermoplastic head mask with standard head-neck rest (HeadSTEP®, IT-V). Patient treatment position was verified by two orthogonal kilovoltage images acquired through a ceiling imaging robot (Siemens, Erlangen, Germany). The analysis of the applied daily corrections during the first treatment week before and after treatment delivery allowed the evaluation of the interfraction and intrafraction reproducibility of the thermoplastic mask, respectively. Concerning interfraction reproducibility, translational and rotational systematic errors (Σs) were ≤2.2 mm and 0.9°, respectively; translational and rotational random errors (σs) were ≤1.6 mm and 0.6°, respectively. Regarding the intrafraction accuracy translational and rotational Σs were ≤0.4 mm and 0.4°, respectively; translational and rotational σs were ≤ 0.5 mm and 0.3°, respectively. Concerning the time-intrafraction displacements correlation Pearson coefficient was 0.5 for treatment fractions with time between position checks less than or equal to median value, and 0.2 for those with time between position controls longer than the median figure. These results suggest that intrafractional patient motion is smaller than interfractional patient motion. Moreover, we can state that application of different imaging verification protocols translate into a relevant difference of accuracy for the same immobilization device. The magnitude of intrafraction displacements correlates with the time for short treatment sessions or during the early phase of long treatment delivery.

Keywords: accuracy; immobilization systems; image-guided radiation therapy; particle therapy

INTRODUCTION

To date advanced conformal radiotherapy techniques such as fractionated stereotactic radiotherapy and radiosurgery as well as intensity-modulated radiotherapy are exploited into clinical routine in order to improve dose conformation without increasing the toxicity [1, 2].

The typical steep dose gradients of these high-precision techniques require high-quality patient fixation and positioning as well as improved treatment verification imaging to minimize the geometric uncertainties and ensure an accurate dose delivery.

Combinations of treatment delivery with online imaging (so-called image-guided radiation therapy: IGRT) likely provide the most effective tool for patient setup control. However, in the treatment chain of IGRT, highest precision and accuracy of all components (i.e. planning, patient positioning, verification imaging, and treatment delivery) are required.

In order to achieve the necessary high degree of accuracy and reproducibility different immobilization systems have been employed for irradiation of head-and-neck, brain and skull base tumors: some institutions have used thermoplastic masks [3–5], others have developed vacuum dental cast systems [6, 7], and still others have employed dental fixations in conjunction with head masks [8, 9]. Implanted fiducial markers have also been tested [10, 11]. Such studies are difficult to compare due to the employment of different methods and measurement of deviations. Despite the advantages advocated by the authors most of them seem equally effective, with reported daily setup errors ranging between 0.5–1 mm in the best series [12].

Currently, there is a growing interest in particle therapy with protons and ions [13]: their distinct physical properties allow a finite range in tissues with particles mostly stopping in the target with almost no exit dose. These features translate into the possibility of high tumor dose deposition while sparing normal surrounding tissues. Moreover, in the case of ions the biologic advantage due to an increased relative biological effectiveness (RBE) can further improve the therapeutic ratio. As in conventional photon radiotherapy the lack of accuracy can lead to a substantial translation or blurring of the delivered dose [14, 15]. However, the sharp dose fall-off and a greater sensitivity to some factors (such as density heterogeneities and/or complex anatomy, computed tomography artefacts and patient positioning errors) [16, 17] can accentuate the effects of the corresponding dose perturbation. These considerations increase both the need for and the relevance of accurate dose administration in particle therapy. Depending on the timing of setup verification, two types of displacements can be assessed: the inter- and intrafraction shifts. Their magnitude may affect in a different way the assessment of appropriate setup margin.

In the present paper we report and discuss the results concerning both the inter- and intrafraction accuracy evaluation of the immobilization system employed in patients with head-and-neck, brain and skull base tumors at our particle therapy center. Moreover, we investigated the influence of intrafraction time on positioning displacements.

MATERIALS AND METHODS

Patient selection

Eligible cases for this analysis included patients with head-and-neck, brain and skull base tumors treated with active beam scanning carbon ion radiotherapy at Heidelberg Ion Therapy Center. For interfraction evaluation all the patients harboring these kinds of tumors would have been eligible. However, for intrafraction analysis we aimed to select cases representative of worst-case setup variation. Assuming that the longer the time of treatment fraction the higher the risk of intrafraction displacements we included patients with expected treatment delivery times >20–25 min. The number of beam spots necessary to irradiate the tumor volume was chosen as the selection criteria, assuming that the higher the number of beam spots the longer the irradiation time (hence, the higher the risk of intrafraction displacements as well). Ultimately, we selected only patients with a number of spots >10 000 at least for one beam (corresponding to a median beam-on time of about seven min). Also, patients with some beams <10 000 and some beams >10 000 spots were included.

The study population consisted of a total of 41 patients treated between January and July 2011. The patient sample included several types of tumor: head-and-neck tumors (20 patients), skull base chordoma and chondrosarcoma (17 patients), low- and high-grade glioma (3 patients), and malignant melanoma (1 patient).

Treatment planning and dose prescription

Computed tomography (CT) imaging for treatment planning was acquired with a 3-mm thickness in spiral modality. Treatment planning was performed on a three-dimensional (3D) CT data cube generated from the CT scan. The target volume was identified on the basis of the co-registered CT and magnetic resonance images.

Depending on the type of the tumor, the treatment was administered either alone or in combination with precision photon radiotherapy. For this reason the number of ion fractions ranged between six and twenty; the dose per fraction was always 3 Gy RBE. Carbon ion therapy was delivered through a horizontal beam line by active beam raster scanning modality [18].

Immobilization system

All the patients were immobilized with a tailored commercial thermoplastic head mask with standard head-neck rest (HeadSTEP®, IT-V) (Fig. 1). This immobilization system was selected based on the results achieved in our previous comparative analysis [19]. However, in that study this device was compared against another one only in terms of interfraction reproducibility.

Positioning, imaging verification and reproducibility assessment

For particle IGRT, the daily patient setup, imaging verification and correction process took place inside the treatment room.

For each fraction, patients were placed on the six degrees of freedom robotic treatment table (Siemens, Erlangen, Germany) (Fig. 1) and the immobilization device was applied. The robotic treatment table has a positioning accuracy of 0.2 mm ± 0.2 mm standard deviation (SD) [19]. Subsequently, the room lasers (defining the reference point of the treatment machine) were aligned with the marks labeled on the mask. During the first fraction we employed the marks defined at the planning CT scan. Then, we

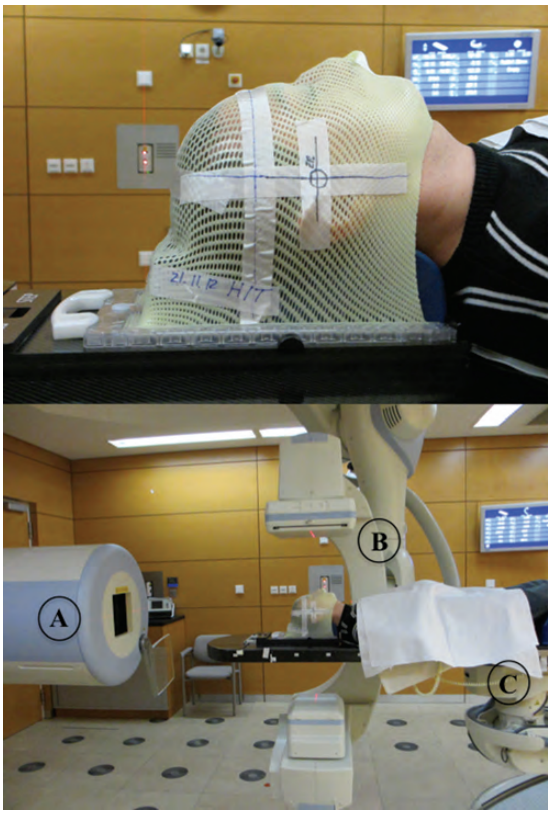

Fig. 1. Immobilization system currently in use at the Heidelberg Ion Therapy Center for head-and-neck, brain and skull base tumors. Top: the system is composed by a tailored commercial thermoplastic mask (HeadSTEP®, IT-V) and a standard head-neck rest. Bottom: treatment room. **A** = horizontal fixed beam line, **B** = ceiling imaging robot, **C** = six degrees of freedom robotic treatment table.

applied the positioning correction according to the treatment planning system (TPS); finally, the updated target point was labeled on the mask so as to correspond to the laser lights. During subsequent treatment fractions, the new marks were used for daily positioning.

After the setup all the procedures were performed with remote control.

For treatment position verification, the room is equipped with a ceiling imaging robot (Siemens, Erlangen, Germany) enabling fluoroscopic as well as X-ray imaging (Fig. 1). The robot-mounted C-arm allows position verification with an accuracy of 0.2 mm ± 0.1 mm [19]. The procedures took place in the following order of succession:

(i) a trained therapist marked anatomically significant structures (such as mastoid processes, nasal septum, dorsum sellae, occipital protuberance etc.) on daily orthogonal radiographs;
(ii) the software accomplished automatic matching so that the landmarks on the portal images were aligned with the corresponding features on the digital reconstructed radiographs (DRRs) obtained from the TPS;
(iii) the therapist or the radiation oncologist manually adjusted the match on-line to achieve the best alignment. It is worth noting that both translational and rotational shifts can be computed;
(iv) the corrections (including rotations) were applied.

Patient position controls were carried out prior to each treatment session and shifts were always corrected.

The analysis of the applied corrections before treatment delivery allowed the evaluation of the interfraction reproducibility of the thermoplastic mask. This evaluation was accomplished by analyzing the data recorded during the first treatment week.

Considering we also aimed to assess the intrafraction accuracy of the immobilization device, for this patient population and during the first treatment week only, the patient position was also verified after the treatment delivery before the patient dismounted: points (i)–(iii) of the above-mentioned workflow were repeated and the corresponding corrections registered and stored.

Both for inter- and intrafraction accuracy evaluation we analyzed the shifts along the medial-lateral, anterior-posterior and cranial-caudal directions, as well as rotational displacements around the vertical, lateral and longitudinal axes. In our coordinate system, the x direction corresponds to the medial-lateral axis of the patient, y to the cranial-caudal axis, and z to the anterior-posterior one. Concerning rotational shifts 'iso' defines the rotation around the vertical axis, 'pitch' rotation around the lateral axis, and 'roll' around the longitudinal axis.

For the evaluation of both inter- and intrafraction errors we used the definitions from van Herk [14]: the distribution of systematic errors (Σ, often called 'treatment preparation' error) was calculated from the SD of individual mean errors. Population random errors (σ, often called 'treatment execution' error or 'day-to-day' error) were assessed from the mean of individual SDs.

For each patient we also evaluated the 3D displacement as follows:

$$\text{3D displacement} = \left(\sum_{1}^{n} x^2 + y^2 + z^2\right)/n$$

where x, y and z are the displacements along the corresponding axis for a certain verification, and n is the number of verifications for the considered patients (in this formula 'Σ' means 'the sum from 1 to n' and does not refer to the systematic error). The overall 3D displacement of the immobilization system was determined as the mean of

individual mean values. This was done for inter- and intrafraction accuracy.

Finally, we investigated the influence of intrafraction time on positioning displacements: all the time intervals between the position verifications (before and after treatment delivery) were correlated with the corresponding magnitude of intrafraction displacements computing the Pearson coefficient.

RESULTS

Interfraction accuracy

The interfraction reproducibility of the immobilization device was assessed by analyzing 418 portal images. Results are detailed in Table 1. Figure 2 depicts the findings as a set of histograms.

Overall, translational shifts ranged from –5.2 to 8.2 mm along the medial-lateral direction (x), between –6.2 and 5.3 mm in the cranial-caudal direction (y), and from –1.6 to 4.5 mm along the anterior-posterior direction (z). The 3D displacement varied between 0.7 and 8.7 mm. The maximum group mean displacement of 1.1 mm was recorded in the anterior-posterior direction (z). Maximum Σ (scored along the medial-lateral direction, x) and σ (registered along the cranial-caudal direction, y) were 2.2 and 1.6 mm, respectively.

Overall, rotational corrections ranged from –2.1 to 4.1º around the vertical axis (iso), between –3.9 and 3.2º around the lateral axis (pitch), and from –4 to 2.5º around the longitudinal axis (roll). The maximum group mean rotation was recorded around the lateral axis (pitch), being 0.3º. Maximum Σ (scored around vertical axis, iso) and σ (registered around both the lateral and longitudinal axis: pitch and roll, respectively) were 0.9 and 0.6º, respectively.

Table 1. Inter- and intrafraction accuracy of the immobilization system: translational, rotational, and three-dimensional displacements

Corrections	Interfraction accuracy			Intrafraction accuracy		
	Group mean	Σ	σ	Group mean	Σ	σ
x (mm)	0.7	2.2	1.3	–0.1	0.3	0.4
y (mm)	–0.1	1.7	1.6	0	0.4	0.5
z (mm)	1.1	1.0	0.6	–0.1	0.3	0.3
iso (°)	0	0.9	0.4	–0.1	0.2	0.3
pitch (°)	0.3	0.8	0.6	0	0.4	0.3
roll (°)	–0.1	0.8	0.6	–0.1	0.3	0.3
3D displacement ± SD (mm)	3.5 ± 1.2	–	–	0.8 ± 0.3	–	–

x = medial-lateral direction, y = cranial-caudal direction, z = anterior-posterior direction, iso = rotation around the vertical axis, pitch = rotation around the lateral axis, roll = rotation around longitudinal axis, 3D = three-dimensional, SD = standard deviation, Σ = systematic error, σ = random error.

Intrafraction accuracy and correlation with delivery time

The intrafraction accuracy of the employed thermoplastic mask was estimated by reviewing 418 portal images. Results are detailed in Table 1. Figure 2 depicts the findings as a set of histograms.

Overall, translational shifts ranged from –2.3 to 1.3 mm along the medial-lateral direction (x), between –2.9 and 1.9 mm in the cranial-caudal direction (y), and from –1.7 to 1.1 mm along the anterior-posterior direction (z). The 3D displacement varied between 0 and 3 mm. The maximum group mean displacement of –0.1 mm was recorded in the medial-lateral direction (x) as well as in the anterior-posterior direction (z). Maximum Σ and σ (both registered along the cranial-caudal direction, y) were 0.4 and 0.5 mm, respectively.

Overall, rotational corrections ranged from –2.5 to 1.3º around the vertical axis (iso), between –1.5 and 3.1º around the lateral axis (pitch), and from –3.2 to 1.6º around the longitudinal axis (roll). The maximum group mean rotation was recorded around both the vertical (iso) and the longitudinal axis (roll), being –0.1º. Maximum Σ (scored around lateral axis, i.e. pitch) and σ (registered around the vertical, lateral, and longitudinal axes: iso, pitch and roll, respectively) were 0.4 and 0.3º, respectively.

Time lapses between the position verifications (before and after treatment delivery) were available in 35 out of 41 patients (177 out of 209 treatment fractions). Median time between position checks was 19 min and 23 s (range, 9 min 48 s to 56 min 19 s). Correlating the time intervals between the position verifications (before and after treatment delivery) with the corresponding magnitude of intrafraction displacements the Pearson coefficient was 0.1, analyzing the entire treatment fractions together (Fig. 3). However, it was 0.5 for treatment fractions with time between position checks ≤19 min 23 s, and 0.2 for those with time between position controls >19 min 23 s.

DISCUSSION

The evaluation of immobilization system accuracy is pivotal for the assessment of geometric errors that take place during the treatment chain (i.e. planning, patient positioning, verification imaging, and treatment delivery). Moreover, such errors should be carefully considered for planning target volume (PTV) design. Geometric uncertainties resulting from patient positioning can be separated into systematic

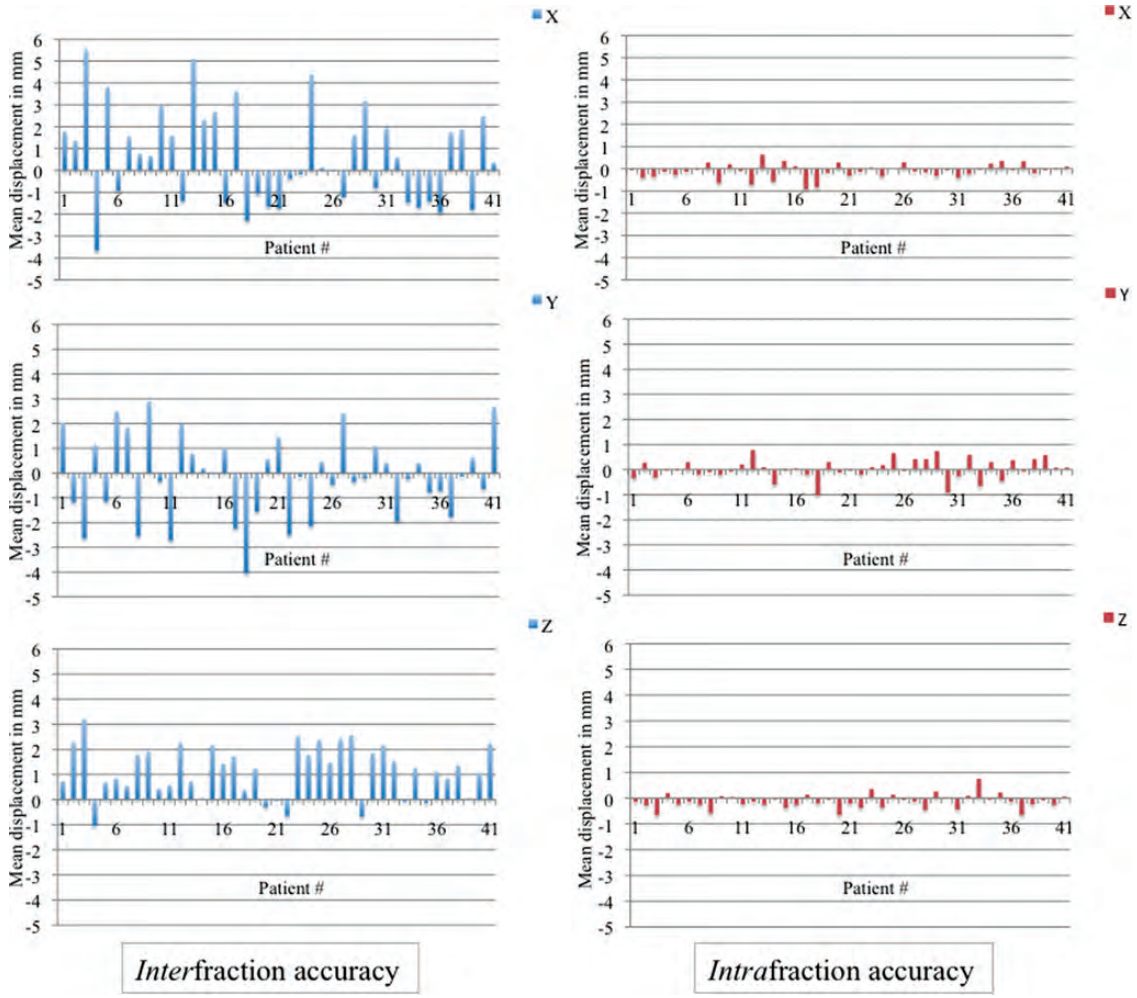

Fig. 2. Mean translational displacement for each patient before (right) and after (left) treatment delivery. x = medial-lateral direction, y = cranial-caudal direction, z = anterior-posterior direction.

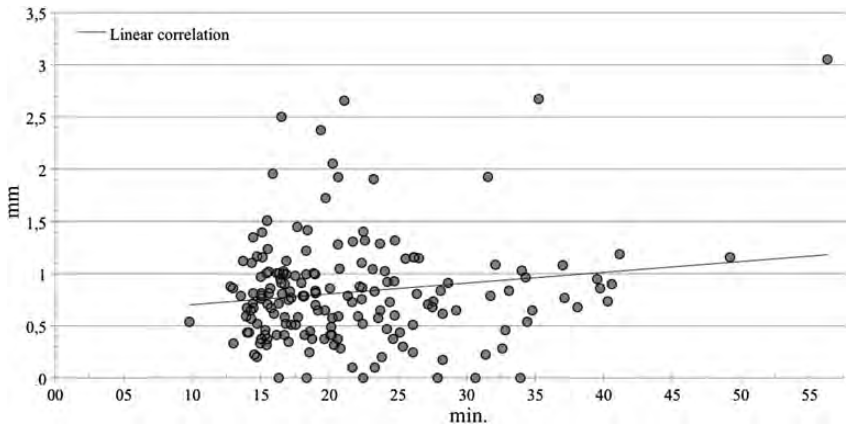

Fig. 3. Pearson correlation of time intervals between the position verifications (before and after treatment delivery) with the corresponding magnitude of intrafraction displacements.

and random displacements [14]. Their effect on the dose distribution is different: the systematic errors influence is the same each fraction leading to a translation of the delivered dose which produces systematic over- and under-dosages; the random errors blur the dose distribution differently day by day, resulting in a smaller absolute effect [14].

In this report we presented a comprehensive analysis of the accuracy achievable with the combination of a commercial thermoplastic mask and daily imaging verifications and corrections for ion beam therapy.

With respect to the group means of each error component, a trend toward a positive cranial-caudal direction (1.1 mm) was observed in interfraction translational displacements. The magnitude of this displacement could be explained taking into account the differences between the simulation and treatment couches as well as the accuracy of the ceiling imaging robot. The remaining error components did not show any trend for both inter- and intrafraction accuracy. These data clearly show that both our treatment preparation chain and the fixation device do not introduce any significant systematic misalignments.

Analysis of daily portal images showed that Σ was ≤2.2 mm and 0.9°, while σ was ≤1.6 mm and 0.6° before the application of daily corrections (interfraction accuracy). Overall, our findings compare favorably with the body of previous reports for thermoplastic immobilization systems with respect to initial setup for similar types of tumors: in general, our data show comparable or less daily initial positioning variability, being the mean 3D displacement of 3.5 mm. In this regard, Boda-Heggemann *et al*. reported a displacement of 4.7 mm [20]; Guckenberg *et al*. pointed out a mean translational vector of 3.2 and 4.6 mm in two thermoplastic systems [21]; Masi *et al.* scored a value of 3.2 mm [22]; Tryggestad *et al*. reported a mean 3D displacement varying between 2.1 and 2.7 mm [5] in four thermoplastic masks. Even though they did not report a translational vector, Bolsi *et al*. pointed out that Σ and σ were ≤2.61 and 3.38 mm [7], respectively. Finally, Velec *et al*. registered a Σ of 1–1.1 mm and 0.6–1.4°, while σ was 1.6–2 mm and 0.8–1.1° in two thermoplastic devices [4].

Analyzing the daily portal images after the treatment delivery (intrafraction accuracy) Σ was ≤0.4 mm and 0.4°, while σ was ≤0.5 mm and 0.3°. Mean 3D displacement was 0.8 mm. Again our findings are consistent with or better than previous reports that have employed thermoplastic masks for tumors with similar anatomical location. Boda-Heggemann *et al*. reported a mean intrafraction 3D displacement of 1.34 mm [20], and Tryggestad *et al*. reported a mean translational vector varying between 0.71 and 1.06 mm [5] in four thermoplastic masks. Even though they did not report a translational vector, Bolsi *et al*. pointed out that intrafraction Σ was ≤2.43 [7]. Finally, Velec *et al*. registered a Σ of 0.7 mm and 0.5°, while σ was 0.8–0.9 mm and 0.7–0.8° in two thermoplastic devices [4].

All these devices feature some benefits such as non-invasive nature, ease of fabrication and quick setup time.

Analyzing the studies that employed a mask with an additional dental tray, our system seems to perform worse in terms of interfraction accuracy. However, the addition of image guidance to our system achieves comparable results. Theelen *et al*. recently provided a comprehensive tabular summary of previously published studies involving thermoplastic masks with an additional dental tray: most series found an accuracy of <2 mm [12].

The abovementioned geometric errors are often considered in treatment planning or PTV design. In fact, according to the International Commision on Radiation Units and Measurements Reports 50 and 62, setup and organ positional uncertainties should be incorporated into the treatment planning process by taking a margin around the clinical target volume (CTV), thereby defining the PTV. Several margin recipes have been published so far. One of the most employed is the formalism provided by van Herk [14], which aims to guarantee that 90% of patients in the population receive a minimum cumulative CTV dose of at least 95% of the prescribed dose. This margin is approximately 2.5 times the Σ plus 0.7 times the σ. For demonstrative and comparative purposes we used this formalism to compute the (idealized) appropriate setup margin based on our results. We neglected rotations in the calculations of the margins. It is noteworthy that this computation accounts only for sources of error determined in our study. It does not account for other types of errors such as planning image registration, target delineation errors, and target motion. In order to detect and quantify the difference between inter- and intrafraction variability, we simulated two radiotherapy protocols:

(i) portal imaging setup verification before delivery of the first treatment session, with subsequent fractions delivered after setup to isocenter marks using room lasers only;
(ii) daily portal imaging and setup corrections as in our current clinical practice.

It is our opinion that such protocols can be representative of the worst and the best correction strategy, respectively. Results are summarized in Table 2.

Considering these data as a whole, it is noteworthy that intrafractional patient motion seems to be smaller than interfractional patient motion, indicating that our immobilization device is better at maintaining a certain patient position than at reproducing this position. Moreover, we can state that the application of different imaging verification protocols translate into a relevant difference of accuracy for the same immobilization device: specifically, the use of a daily IGRT protocol yields a significant reduction in both systematic and random errors. As a consequence, the strategy for PTV design can also be optimized and improved, ultimately translating into a better therapeutic ratio. This is of great relevance when there are steep dose gradients in the proximity of healthy structures, as in sophisticated photon techniques and even more so in particle therapy where other sources of uncertainties (such as particle

Table 2. Simulation of margins calculation for two corrections protocols employing the inter- and intrafraction variability

Geometric errors	Interfraction variability			Intrafraction variability		
	x (mm)	*y* (mm)	*z* (mm)	*x* (mm)	*y* (mm)	*z* (mm)
Σ	2.2	1.7	1.0	0.3	0.4	0.3
σ	1.3	1.6	0.6	0.4	0.5	0.3
Correction protocol	Protocol 1[a]			Protocol 2[b]		
	x (mm)	*y* (mm)	*z* (mm)	*x* (mm)	*y* (mm)	*z* (mm)
PTV margins	6.4	5.4	2.9	1.0	1.3	1.0

x = medial-lateral direction, *y* = cranial-caudal direction, *z* = anterior-posterior direction, Σ = systematic error, σ = random error, PTV = planning target volume. [a]Protocol 1: portal imaging setup verification before delivery of the first treatment session with subsequent fractions delivered after setup to isocenter marks using room lasers only. [b]Protocol 2: daily portal imaging and setup corrections (as in our current clinical practice).

scattering in complex anatomy and computed tomography artifacts) have to be taken into account during the treatment planning and delivery [16, 17]. Such findings are consistent with data reported by other authors [4, 5, 7, 20]. Finally, it is of note that a high level of accuracy can be achieved by employing the combination of an IGRT protocol with a commercial thermoplastic mask, the benefits of which include its noninvasive nature, ease of fabrication and quick setup time. These data suggest that thermoplastic masks can perform as well as those used for stereotactic radiotherapy when combined with image guidance.

The last issue we addressed was the influence of intrafraction time on positioning displacements. To date, only a few authors have focused on this topic and their results are not consistent each other. Hoogeman *et al*. [23] reported that the magnitude of intrafraction Σ of a similar immobilization device employed for cranial treatments strongly correlated with time following initial positioning ($r = 0.91$) for time lapses ranging between 0 and 15 min. For the same time range, the group mean error remained small and σ slightly increased [23]. Conversely, Tryggestad *et al*. concluded that there was minimal evidence that the magnitude of intrafraction movements is correlated with the time between the pre- and post-treatment setup verification (maximum $r = 0.30$) [5]. The mean time difference between cone-beam scans ranged from 16.67–21.16 min. Correlating the time intervals between the position verifications (before and after treatment delivery) with the corresponding magnitude of intrafraction displacements (analyzing all of the treatment fractions together) our Pearson coefficient was 0.1. Based on this result we should also conclude that our data suggest a very weak correlation between time and intrafraction misalignments. However, when we split the data according the median time (19 min 23 s) between the verification images we found that the Pearson coefficient was 0.5 (moderate correlation) for treatment fractions with time between position checks less than or equal to the median value, and 0.2 (weak correlation) for those with time between position controls > 19 min 23 s. These findings may have arisen because our time lapse ranged between 9 min 48 s and 56 min 19 s, i.e. we monitored patients longer than in previous published series, as one might assume that after the positioning patients start relaxing, producing displacements the magnitude of which correlates with time. This seems to occur both in short treatments sessions and in the early phase of long treatment sessions. If the treatment session lasts about 19 min the correlation is still valid at the end of treatment; however, for treatments lasting more than about 19 min, the process reaches a plateau and then the misalignments lose their correlation with time. From this standpoint, our findings compare favorably with Hoogeman *et al*. [23] who reported a linear time-intrafraction displacements correlation within the time range of ~ 15 min.

ACKNOWLEDGEMENTS

Part of the data has been presented as a poster at 50th Meeting of the Particle Therapy Co-Operative Group (PTCOG), May 8–14, 2011, Philadelphia, USA. The PTCOG scientific board awarded the poster with a travel fellowship. We thank Francesco Fellin (ATreP) for helping us with the graphical representation of the data.

FUNDING

This work was supported by the European community in the seventh frame work program, 2007–2012 PARTNER Project, [grant agreement n° 215840-2], as well as the Klinische Forschergruppe Schwerionentherapie KFO 214.

REFERENCES

1. Combs S-E, Welzel T, Schulz-Ertner D *et al*. Differences in clinical results after LINAC-based single-dose radiosurgery versus fractionated stereotactic radiotherapy for patients with

vestibular schwannomas. *Int J Radiat Oncol Biol Phys* 2010;**76**:193–200.
2. Amelio D, Lorentini S, Schwarz M *et al*. Intensity-modulated radiation therapy in newly diagnosed glioblastoma: a systematic review on clinical and technical issues. *Radiother Oncol* 2010;**97**:361–9.
3. Fuss M, Salter B-J, Cheek D *et al*. Repositioning accuracy of a commercially available thermoplastic mask system. *Radiother Oncol* 2004;**71**:339–45.
4. Velec M, Waldron J-N, O'Sullivan B *et al*. Cone-beam CT assessment of interfraction and intrafraction setup error of two head-and-neck cancer thermoplastic masks. *Int J Radiat Oncol Biol Phys* 2010;**76**:949–55.
5. Tryggestad E, Christian M, Ford E *et al*. Inter- and intrafraction patient positioning uncertainties for intracranial radiotherapy: a study of four frameless, thermoplastic mask-based immobilization strategies using daily cone-beam CT. *Int J Radiat Oncol Biol Phys* 2011;**80**:281–90.
6. Sweeney R, Bale R, Vogele M *et al*. Repositioning accuracy: comparison of noninvasive head holder with thermoplastic mask for fractionated radiotherapy and a case report. *Int J Radiat Oncol Biol Phys* 1998;**41**:475–83.
7. Bolsi A, Lomax A-J, Pedroni E *et al*. Experience at Paul Scherrer Institute with a remote patient positioning procedure for high-throughput proton radiation therapy. *Int J Radiat Oncol Biol Phys* 2008;**71**:1581–90.
8. Baumert B-G, Egli P, Studer S *et al*. Repositioning accuracy of fractionated stereotactic irradiation: assessment of isocentre alignment for different dental fixations by using sequential CT scanning. *Radiother Oncol* 2005;**74**:61–6.
9. Minniti G, Valeriani M, Clarke E *et al*. Fractionated stereotactic radiotherapy for skull base tumors: analysis of treatment accuracy using a stereotactic mask system. *Radiat Oncol* 2010;**5**:1.
10. Jones D, Christopherson D-A, Washington J-T *et al*. A frameless method for stereotactic radiotherapy. *Br J Radiol* 1993;**66**:1142–50.
11. Kim K-H, Cho M-J, Kim J-S *et al*. Isocenter accuracy in frameless stereotactic radiotherapy using implanted fiducials. *Int J Radiat Oncol Biol Phys* 2003;**56**:266–73.
12. Theelen A, Martens J, Bosmans G *et al*. Reloctable fixation systems in intracranial stereotactic radiotherapy. Accuracy of serial CT scans and patient acceptance in a randomized design. *Strahlenther Onkol* 2012;**188**:84–90.
13. Nyström H, Blomqvist E, Høyer M *et al*. Particle therapy – a next logical step in the improvement of radiotherapy. *Acta Oncol* 2011;**50**:741–4.
14. van Herk M. Errors and margin in radiotherapy. *Semin Radiat Oncol* 2004;**14**:52–64.
15. Gensheimer M-F, Yock T-I, Liebsch N-J *et al*. *In vivo* proton beam range verification using spine MRI changes. *Int J Radiat Oncol Biol Phys* 2010;**78**:268–75.
16. Lomax A-J. Intensity modulated proton therapy and its sensitivity to treatment uncertainties 2: the potential effect of calculational uncertainties. *Phys Med Biol* 2008;**53**: 1027–42.
17. Lomax A-J. Intensity modulated proton therapy and its sensitivity to treatment uncertainties 2: the potential effect of inter-fraction and inter-field motions. *Phys Med Biol* 2008; **53**:1043–56.
18. Haberer T, Becher W, Schardt D *et al*. Magnetic scanning system for heavy ion therapy. *Nucl Instr Meth Phys Res* 1993;**330**:296–305.
19. Jensen A-D, Winter M, Kuhn S *et al*. Robotic-based carbon ion therapy and patient positioning in 6 degrees of freedom: setup accuracy of two standard immobilization devices used in carbon ion therapy and IMRT. *Radiat Oncol* 2012;**7**:51.
20. Boda-Heggemann J, Walter C, Rahn A *et al*. Repositioning accuracy of two different mask systems 3D revisited: comparison using 3D/3D matching with cone-beam CT. *Int J Radiat Oncol Biol Phys* 2006;**66**:1568–75.
21. Guckenberger M, Baier K, Guenther I *et al*. Reliability of the bony anatomy in image-guided stereotactic radiotherapy of brain metastases. *Int J Radiat Oncol Biol Phys* 2007; **69**:294–301.
22. Masi L, Casamassima F, Polli C *et al*. Cone beam CT image guidance for intracranial stereotactic treatments: comparison with a frame guided set-up. *Int J Radiat Oncol Biol Phys* 2008;**71**:926–33.
23. Hoogeman M-S, Nuyttens J-J, Levendag P-C *et al*. Time dependence of intrafraction patient motion assessed by repeat stereoscopic imaging. *Int J Radiat Oncol Biol Phys* 2008; **70**:609–18.